Jurnal Kejuruteraan 38(7) 2026: 3239-3249
https://doi.org/10.17576/jkukm-2026-38(7)-06

Effect of Ferromagnetic Material Composition on Magnetic Flux Leakage Signal Behavior During Carbon Steel Cyclic Testing

Azli Arifin*, Shahrum Abdullah, Salvinder Singh Karam Singh & Ahmad Kamal Ariffin

Department of Mechanical and Manufacturing Engineering, Faculty of Engineering and Built Environment,,

Universiti Kebangsaan Malaysia, UKM Bangi, Selangor, Malaysia.

**Corresponding author: azli@ukm.edu.my*

Received 7 November 2025, Received in revised form 10 June 2026
Accepted 10 July 2026, Available online 30 October 2026

ABSTRACT

Fatigue cracks in steel structures pose a significant risk of failure if not detected early or managed properly. Metal Magnetic Memory (MMM) testing, which relies on detecting variations in the self-magnetic leakage field (SMLF), is a commonly applied non-destructive technique for crack detection and monitoring. However, a limited understanding of how SMLF evolves under cyclic loading conditions presents a challenge in improving the reliability of MMM testing. To enhance the precision of fatigue crack detection in steel structures, it is essential to explore the relationship between SMLF behaviour and loading conditions. In particular, studying how differences in ferromagnetic material composition affect MMM signals can provide valuable insights for improving structural health monitoring. This research focuses on examining MMM signal responses during fatigue crack propagation in carbon steels with varying ferromagnetic compositions. The study also aims to correlate these MMM responses with crack dimensions. A constant amplitude cyclic loading approach was applied, and an MMM scanning instrument was used to measure the SMLF signals. Three types of pre-cracked carbon steel specimens: ASSAB 705, ASSAB 709 and ASSAB 760, were tested at stress ratios (R) of 0.1 and 0.3. SMLF data were then assessed in correspondence with the quantified ferromagnetic content in each material. The findings demonstrate that the constants in the fitted exponential model differ based on the ferromagnetic composition of the steel, highlighting the influence of material properties on MMM signal characteristics.

Keywords: Magnetic flux gradient; fatigue crack growth; crack detection

INTRODUCTION

Steel remains a preferred material across numerous sectors, including construction and transportation, due to its high strength and long-term durability. Despite these advantages, steel components are prone to fatigue cracks as they undergo repeated loading, which can eventually lead to structural failures if left unaddressed. To maintain the structural integrity and safety of such systems, non-destructive testing (NDT) methods are essential for detecting and tracking crack development. Among these techniques, Metal Magnetic Memory (MMM) testing has emerged as a promising tool. This method detects anomalies in ferromagnetic materials, particularly steel, by measuring variations in the self-magnetic leakage field (SMLF), which can signal the presence and progression of fatigue cracks. (Ariffin et al. 2015; Firdaus et al. 2023). Quantitative assessment through the stress concentration stage using the MMM method can be conducted while scanning along the material surface, using the analysis of the variation per distance of the normal or tangential magnetic flux signal parameters applied to the identification of stress concentration zones (Dubov, 2006; Dubov et al. 2020). The distribution of peak anomalies in magnetic flux signal amplitude was analysed to determine regions of stress concentration, with the highest gradient value indicating the location of the most intense stress concentration (Liu et al. 2023). Building on this approach, Mutalib et al. (2025) identified defective regions in the steel reinforcement of concrete structures, correlating these defects with areas of elevated stress.

Initially, Dubov (1997) introduced the Metal Magnetic Memory (MMM) technique as a novel approach for high

stress areas detection in ferromagnetic materials. His early work focused on tension tests and investigations on gas pipelines subjected to light loads, demonstrating the method's potential for identifying zones susceptible to fatigue damage (Dubov et al. 2002). Building on this foundation, Shen, Wu, and Wang (2004) extended the application of MMM to pressure vessels, particularly examining how magnetic signals change in weld regions under light cyclic loading conditions. Their research highlighted the sensitivity of MMM in detecting early signs of structural weakness in critical components. Following these initial studies, researchers further developed MMM by establishing quantitative relationships between magnetic memory signals, applied load, and crack characteristics. Significant contributions were made by Lihong et al. (2008), Ni et al. (2018) and Huang et al. (2014a) who refined the theoretical models and experimental approaches to better interpret MMM data for crack detection and monitoring.

More recently, Zhang et al. (2020) advanced the field by developing a nonlinear magneto-mechanical constitutive model specifically for ferromagnetic materials under fatigue loading. Their model incorporated the effects of plastic deformation and complex stress-strain behaviours, enabling more accurate predictions of magnetic responses during crack initiation and propagation. This progression reflects the growing sophistication of MMM techniques as powerful tools for structural health monitoring.

Despite the advancements, MMM testing still faces challenges in understanding its underlying mechanisms, particularly under cyclic loading conditions. The complex interaction between cyclic stress and magnetic domain realignment in ferromagnetic materials remains inadequately described. The limited understanding of this phenomenon affects the precision of MMM testing in detecting and characterising fatigue cracks in steel structures. Furthermore, the potential impact of different ferromagnetic material compositions on MMM signal behaviour raises concerns about the reliability of crack detection methods used to ensure the structural soundness of steel components. This study seeks to examine how MMM signals respond during fatigue crack propagation in carbon steels with varying ferromagnetic compositions and to evaluate the relationship between these signals and crack dimensions. A better understanding of these interactions may lead to improved calibration procedures and more accurate interpretation of MMM signal anomalies in real-world applications.

METHODOLOGY

MATERIALS

This study utilised 3 mm thick carbon steel specimens: ASSAB 705, ASSAB 709 and ASSAB 760, which are commonly employed in machinery applications (Li et al., 2001; Hou et al., 2022; Anggraini, 2017). These materials were selected for their distinct magnetic properties, particularly due to the differing contents of magnetic elements such as Nickel (Ni) and Chromium (Cr). These elements influence magnetic domain behavior, which directly affects the accuracy of MMM signal interpretation. The specific chemical compositions of the selected carbon steels are outlined in Table 1. The material selection ensures that the results are relevant for practical engineering applications involving structural fatigue and magnetic-based diagnostics.

TABLE 1. Composition details of tested carbon steel grades

Materials	Chemical compositions, in wt.%		
	C	Cr	Ni
ASSAB 705	0.35	1.40	1.40
ASSAB 709	0.48	1.10	
ASSAB 760	0.50	-	-

TABLE 2. Mechanical characteristics of the tested steels

Steels :	ASSAB705	ASSAB709	ASSAB760
Modulus of elasticity (GPa)	201.3	200.1	197.1
Yield strength, (MPa)	837.6	832.8	417.0
Ultimate strength (MPa)	982.7	1043.0	747.2

EXPERIMENT DESIGN AND PROCEDURE

Tensile and cyclic tests were conducted using a universal testing machine, the 100 kN INSTRON 8801, to evaluate the mechanical behaviour of the steel specimens. The tensile test specimens were fabricated according to ASTM E8M-01 standards, ensuring consistent geometry and reliable data for material characterization, and the mechanical properties are provided in Table 2. Single-edge crack compact tension (CT) specimens were fabricated for fatigue crack growth experiments following the guidelines of ASTM E647-00, as shown in Figure 1. Special attention was given to machining precision to maintain dimensional accuracy and minimize variations that could affect the mechanical response during testing. Prior to initiating the tests, all specimens underwent careful visual inspection to identify any surface defects or irregularities that might

influence the experimental outcomes. To further enhance surface quality, specimens were polished to a mirror finish using ultra-fine abrasive papers and polishing compounds. This mirror polishes minimized surface roughness and eliminated microscopic scratches, ensuring a defect-free surface essential for accurate fatigue testing and reliable magnetic signal measurements (Sahadan et al. 2021). The specimens underwent a preliminary demagnetisation process based on the principle of alternating field demagnetisation to eliminate residual magnetisation introduced during the manufacturing process.

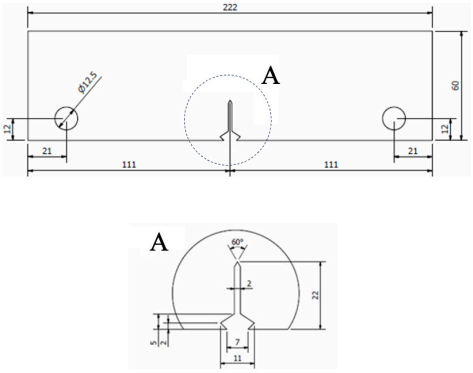


FIGURE 1. Geometry of the CT specimen (unit in mm)

Cyclic loading experiments were performed to analyze the fatigue crack propagated behaviour of the selected steel materials under controlled stress ratios of R = 0.1 and 0.3. A constant load range of 4 kN was applied during the tests, with a frequency set at 10 Hz to simulate realistic cyclic loading conditions typically experienced in engineering structures (Arifin et al. 2022). Throughout the fatigue testing, two critical types of data were continuously recorded. The first dataset consisted of fatigue crack growth measurements obtained using a Crack Opening Displacement (COD) device, as illustrated in Figure 2(a), which allowed for precise monitoring of crack length and opening displacement during cyclic loading. The second dataset involved capturing magnetic flux leakage signals generated by the specimens under stress, detected using a TSCM-2FM scanning device shown in Figure 2(b). These simultaneous measurements enabled correlation between mechanical crack growth and magnetic signal variation, providing insights into the effectiveness of Metal Magnetic Memory (MMM) techniques for early crack detection and structural health monitoring. Prior to testing, the specimen geometry parameters were entered into the crack growth software interfaced with INSTRON 8801 machine software, as shown in Figure 2(c). Using predefined specimen geometry and the real-time COD measurements, the software automatically determines the crack length.

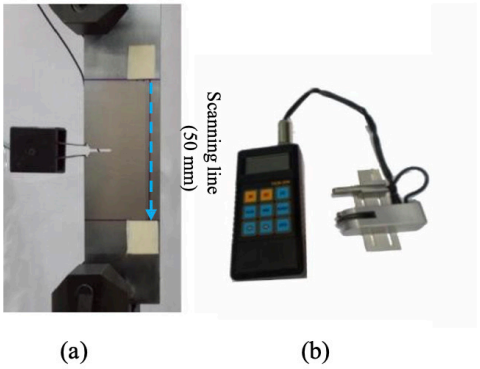


FIGURE 2. Experimental setup (a) Specimen with COD; (b) TSCM-2FM (c) Crack growth software

The magnetic flux sensor was mounted on a sensor wheel, which guided its movement along a predefined scanning path, as illustrated in Figure 2(a). The notch was accurately aligned at the center of this path, ensuring consistent positioning during each scan. The observation line was placed 10 mm away from the edge opposite the notched side. SMLF data were continuously recorded starting from the initiation of the test, beginning at the pre-existing crack length until the specimen became unstable due to crack propagation. Throughout the test, the sensor maintained constant contact with the specimen surface to ensure consistent signal quality. Signal acquisition was synchronised with the loading cycles to detect subtle changes in magnetic flux distribution related to crack advancement. This approach allowed for a detailed correlation between mechanical crack development and variations in magnetic response, providing insight into the early detection capability of MMM for fatigue damage assessment in steel components.

RESULTS AND DISCUSSION

Two types of plots were produced from the experimental results; the SMLF signal plot (H) and the SMF gradient plot of H (dH/dx). The behaviour of the SMLF signals intensity were thoroughly examined by recognising the

normal component of the magnetic flux signal, H, which captures the variations in intensity occurring during cyclic loading. This value was obtained through magnetic flux signal analysis using the MMM-System 3.0 software. Figure 3 illustrates representative patterns of the H signals recorded during the MMM data acquisition, showing the H signal plotted as a function of the scanning track length (Lx) across a total span of 50 mm. As the sensor traverses the region between Lx = 105 and 115 mm, corresponding to the vicinity of the crack tip, a localized "ditch" is observed in the H signal. This phenomenon is attributed to the strong magnetic field caused by stress concentration and magnetic flux leakage around the crack tip, resulting in a sharp variation in the measured H signal.

The magnetic flux leakage signal, Hp2, was recorded when the cyclic load was first applied at the beginning of the fatigue test, representing the initial state of the specimen before significant crack growth occurred. As the number of test cycles increased, the magnetic flux signal gradually intensified, as demonstrated by the Hp4 line, which corresponds to an intermediate stage of crack propagation. This increase in the magnetic signal continued and became more pronounced, as shown by the Hp6 line, which corresponds to a later stage where the crack size had grown substantially. The observed escalation in magnetic flux leakage signals with increasing fatigue cycles and crack length indicates a strong and consistent correlation between magnetic signal intensity and the progression of fatigue crack propagation in the material. Figure 4 shows the final crack paths for ASSAB 705, ASSAB 709 and ASSAB 760 specimens tested under both stress ratios.

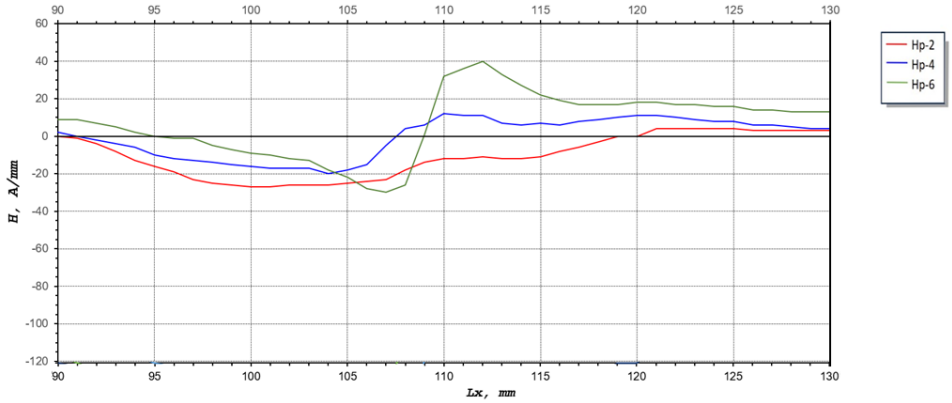


FIGURE 3. Magnetic signal data displayed through the MMM System 3.0 software interface.

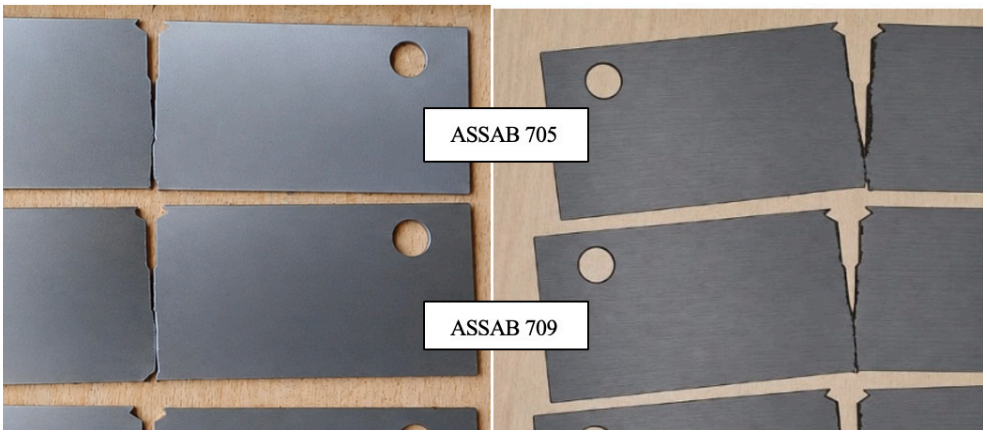


FIGURE 4. Photographs of the tested specimens after fatigue failure, illustrating the final crack paths for ASSAB 705, ASSAB 709, and ASSAB 760 steels under cyclic loading for stress ratio R=0.1 and R=0.3.

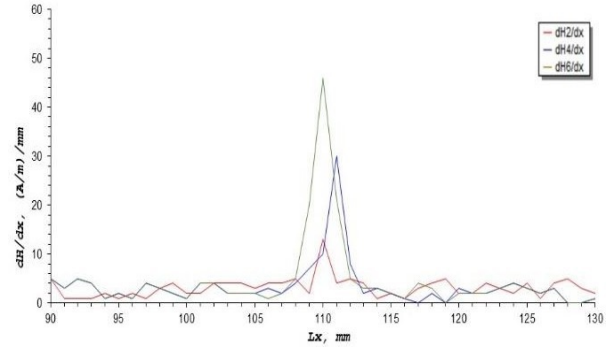
The gradient graph, dH/dx, was also essential for identifying zones of stress concentration. Sharp changes in this gradient are often associated with crack tips or locations undergoing significant plastic deformation. By comparing multiple stages of cyclic loading, the evolution of stress concentration could be tracked, offering a non-invasive means to predict crack advancement. It is important to note that the values of the SMLF signal, H,

measured in the vicinity of machine components are notably influenced by external magnetic field effects on the components, according to Zhou et al. (2019). Therefore, background magnetic interference was minimised through proper shielding and calibration before each measurement session. The ability to monitor the progression of H and its gradient over time provides critical insight into the reliability of MMM testing as a predictive tool for structural failure in ferromagnetic materials.

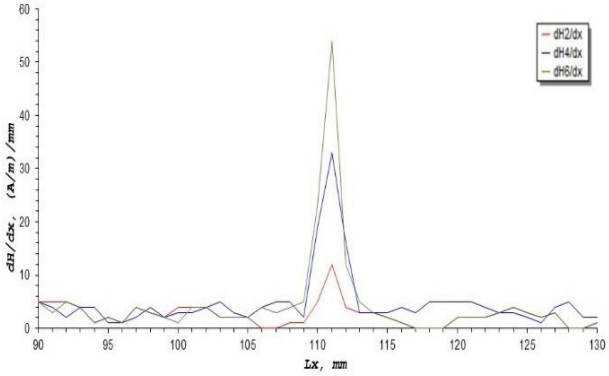
Figures 5 to 7 show the amplitude variations of the dH/dx signals corresponding to crack lengths of 5 mm, 10 mm and 15 mm in the steel samples, denoted as dH2/dx, dH4/dx, and dH6/dx, respectively. The peak values of the dH/dx signal demonstrate the gradient values of the H signal. The figures also show that the increase in crack length prompted a rise in the peak value of the dH/dx signals within the stress concentration region. This indicates that no significant changes were detected in the SMLF signal with increasing distance from the crack region. Additionally, observations showed that for all steel grades and stress ratios (R), the peak dH/dx amplitude was consistently recorded at distances (Lx) of 24–26 mm, which closely corresponds to the location of the crack in the specimen.

Moreover, Zhang et al. (2012) and Ahmad et al. (2015) examined the stress concentration zones responsible for initiating fatigue cracks in steel specimens subjected to cyclic loading. Similarly, Huang et al. (2014a, 2014b) observed a consistent increase in dH/dx signal values with the progression of crack length across two different specimen geometries. This rise in dH/dx was associated with the enhanced intensity of H values within the crack region.

Throughout the fatigue crack growth tests, dH/dx readings were continuously recorded as the crack length progressed in increments of 1 mm. This procedure was repeated until the crack extended to between 18 and 24 mm, at which point the specimen approached a near-failure, unstable state. The test data were subsequently plotted as illustrated in Figure 8. Huang et al. (2016) identified a similar exponential correlation between the magnetic signal gradient and crack length in single-edge notched Q235 low-carbon steel using a three-point bending test. Likewise, Zhang et al. (2021) reported a comparable exponential model for single-edge notched HRB400E steel specimens subjected to cyclic mode I opening tests. Comparison between the a–N (Figure 9) and dH/dx–a (Figue 8) curves reveals a similar exponential growth pattern for all three steels. In the initial stage of fatigue loading, both crack length and dH/dx increase slowly, indicating stable crack initiation and early crack propagation. As fatigue progresses, both curves exhibit an accelerated increase, corresponding to the rapid crack growth region prior to failure.

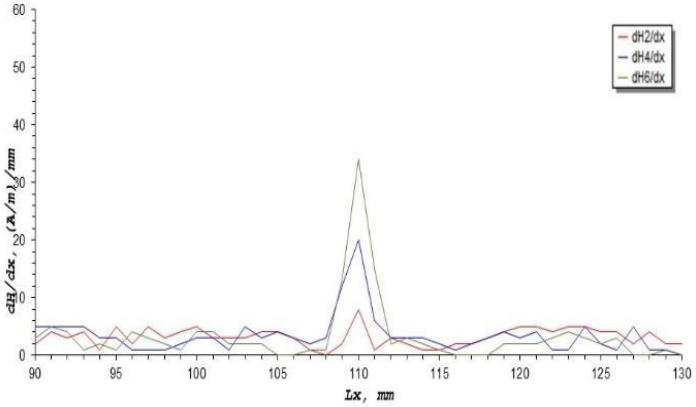


(a)

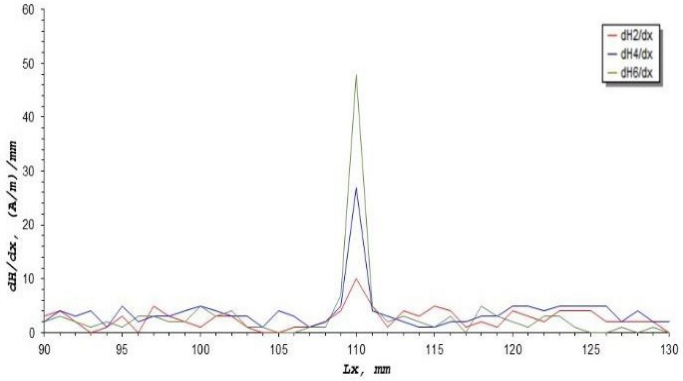


(b)

FIGURE 5. The dH/dx signals for ASSAB705 steel specimens with R: (a) 0.1 (b) 0.3.

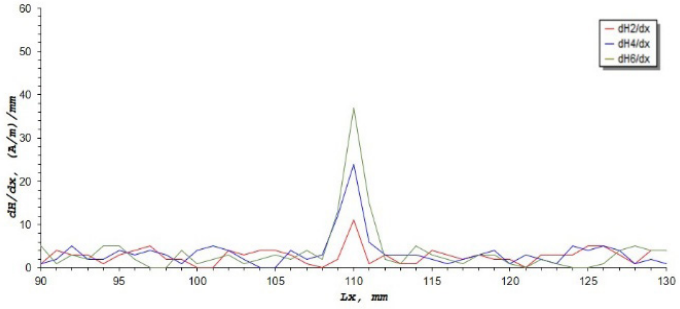


(a)

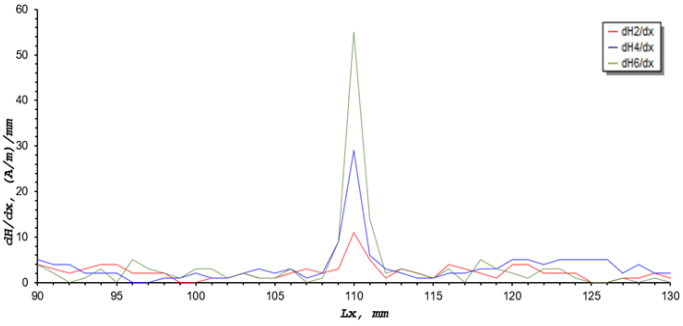


(b)

FIGURE 6. The dH/dx signals for ASSAB709 steel specimens with R: (a) 0.1 (b) 0.3



(a)



(b)

FIGURE 7. The dH/dx signals for ASSAB760 steel specimens with R: (a) 0.1 (b) 0.3

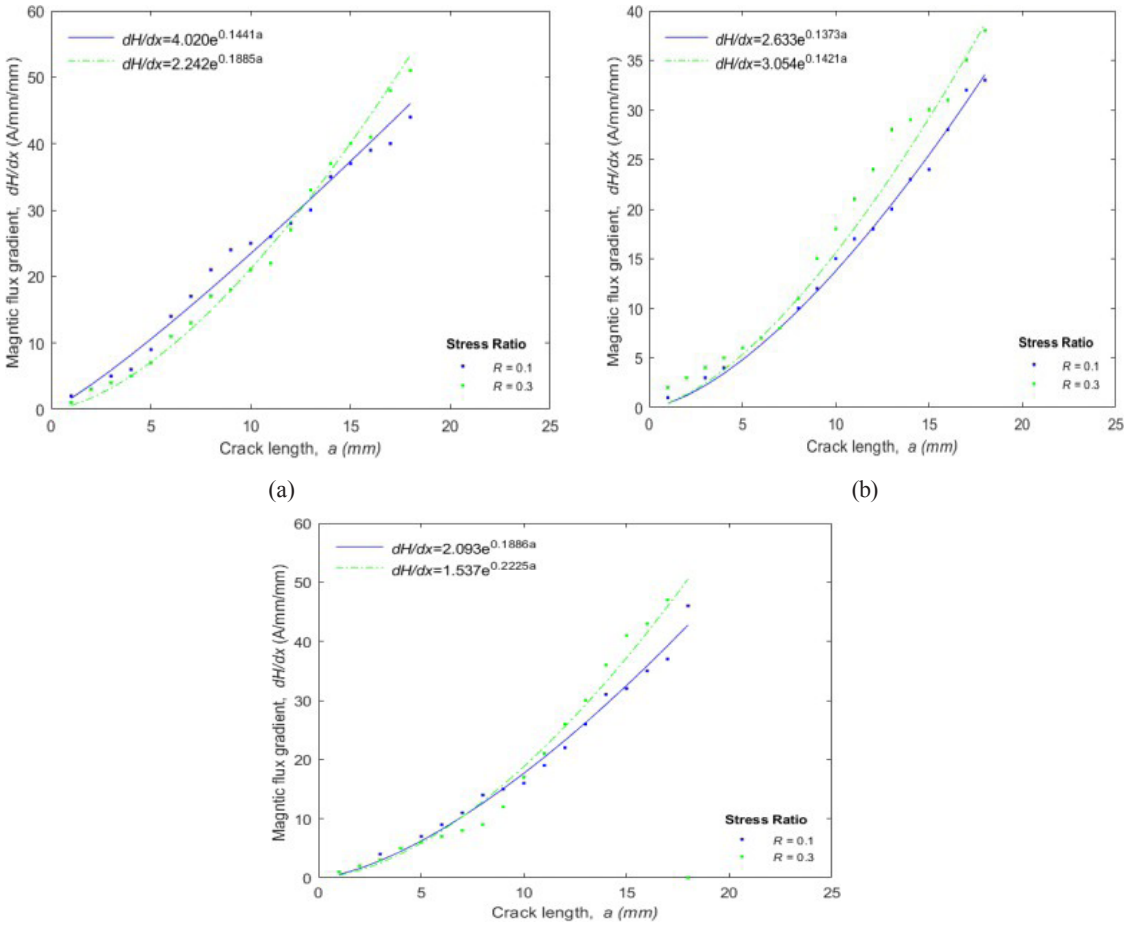


FIGURE 8. The correlation between crack length (a) and magnetic signal gradient (dH/dx) for three types of ASSAB steel: (a) 705, (b) 709, and (c) 760.

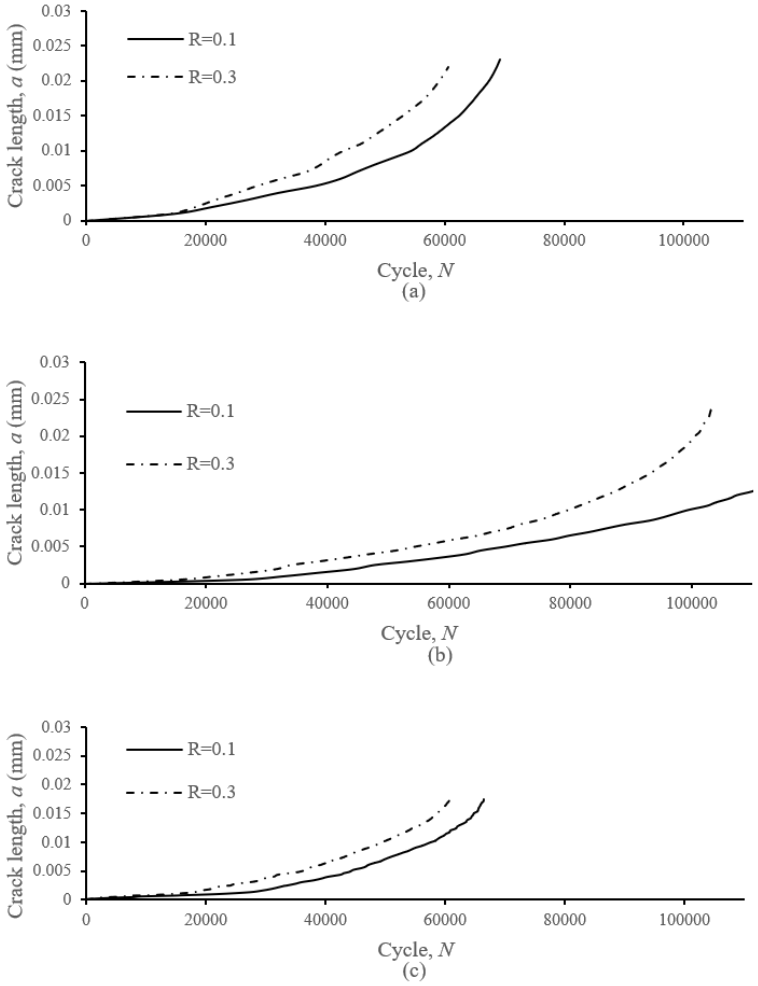


FIGURE 9. Graph showing the correlation between crack length (a) and cycle (dH/dx) for three types of ASSAB steel: (a) 705, (b) 709, and (c) 760.

TABLE 3. Exponent m values for ASSAB 705, ASSAB 709 and ASSAB 760 steel materials

Materials	Chemical compositions (wt.%)			Exponent m	Exponent m
	C	Cr	Ni	(R = 0.1)	(R = 0.3)
ASSAB 705	0.35	1.40	1.40	0.1441	0.1885
ASSAB 709	0.48	1.10	-	0.1373	0.1421
ASSAB 760	0.50	-	-	0.1886	0.2225

The consistent trend of increasing dH/dx amplitude with crack progression provides critical insights into the feasibility of using MMM as a reliable crack growth monitoring technique. The gradient component, dH/dx, serves as a sensitive indicator for localised magnetic field variations caused by material discontinuities. As the crack grows, the redistribution of stress fields induces significant magneto-mechanical effects that are captured through the MMM response. These results suggest that dH/dx signals not only reflect the presence of fatigue cracks but can also serve as a diagnostic parameter for predicting the crack propagation rate. By establishing a quantitative relationship between the gradient signal and crack length, engineers can potentially estimate the remaining life of structural components with greater accuracy. This predictive capability is particularly valuable in industries such as aerospace, automotive, and civil infrastructure, where early crack detection and condition-based maintenance are

crucial for ensuring operational safety and reducing unexpected downtime. In future studies, combining MMM data with finite element simulations could further refine the crack growth models and support the development of automated monitoring systems that integrate magnetic sensing with real-time fatigue diagnostics.

As illustrated in Figures 7(a) to 7(c), the relationship between the dH/dx signal and the crack length, a, can be accurately described using an exponential model, as expressed in Equation (1):

$$\frac{dH}{dx} = ce^{ma} \quad (1)$$

where *c* represents the initial magnetic gradient and m represents the sensitivity of magnetic signal with crack growth. The parameter m depends on material composition, magnetic permeability, microstructure and stress ratio. Higher stress ratios increase crack-tip plasticity, whereas alloy composition affects magnetic domain mobility, leading to different *m* values. The higher stress concentration causes magnetic domain redistribution and consequently an exponential increase in dH/dx. Therefore, Equation (1) indirectly quantifies fatigue damage through crack growth.

Table 3 summarises the m values for the ASSAB 705, ASSAB 709, and ASSAB 760 steel materials obtained from the graphs. Based on the data presented in Table 3, chromium (Cr) and nickel (Ni) appear to influence the fatigue exponent (m), although their individual contributions cannot be isolated because the steels also differ in carbon content and other metallurgical characteristics. ASSAB 705, which contains the highest Cr (1.40 wt.%) and Ni (1.40 wt.%) contents, exhibits the lowest m values (0.1441 at R = 0.1 and 0.1885 at R = 0.3), suggesting a lower sensitivity of the parameter to fatigue damage evolution. In contrast, ASSAB 760, which contains neither Cr nor Ni, demonstrates the highest m values (0.1886 and 0.2225), whereas ASSAB 709, with a lower Cr content (1.10 wt.%) and no Ni, exhibits intermediate m values. These observations suggest that increasing Cr and Ni contents may contribute to a reduction in the fatigue exponent; however, this trend should be interpreted with caution because the observed differences may also be influenced by variations in carbon content and other metallurgical factors. The exponential nature of the relationship indicates a rapid increase in the gradient signal as the crack lengthens, reflecting enhanced stress concentration and magnetic perturbation near the crack tip. This behaviour aligns with previous studies on magneto-mechanical effects in ferromagnetic materials. Understanding the m value helps quantify the sensitivity of the MMM signal to fatigue damage in each steel type. Higher m values suggest a more pronounced magnetic response to crack growth, which may be advantageous for early crack detection and condition monitoring applications.

Parameter m represents the correlation between MMM signals and crack propagation in various steels and applied stress ratios. The findings indicate that the sensitivity of MMM signals to stress is not uniform among the tested steels and may vary depending on the stress ratio applied. Certain steel types exhibited a more noticeable response in MMM signal behaviour under higher stress levels, highlighting the influence of both material composition and loading conditions on signal sensitivity. This variation in m reflects differences in the magnetic and mechanical properties of the materials, such as microstructure, hardness, and the presence of alloying elements like Nickel and Chromium. Understanding how m behaves allows for better calibration of MMM systems for specific materials, improving the accuracy of crack detection. It also aids in selecting appropriate materials for structural applications where real-time condition monitoring is required. In practical terms, steels with higher m values may provide more distinct magnetic responses to fatigue crack growth, making them suitable candidates for critical components in safety-sensitive industries. Additionally, monitoring changes in m over time could be used to assess material degradation and predict failure before it occurs.

CONCLUSION

This research examined the behaviour of Metal Magnetic Memory (MMM) signals in various ferromagnetic materials, focusing on carbon steels with different compositions, and explored their correlation with crack length. The findings revealed that the peak value of the magnetic flux gradient signal, dH/dx, within the stress concentration zone increased progressively with crack growth. This indicates that an exponential relationship exists between the dH/dx signal and crack length, a. The constant parameter m serves to quantify this relationship, reflecting differences in material response across the various steel types and their sensitivity to varying stress ratios, particularly under higher loading conditions. The exponential parameter (m), which characterizes the growth rate of the magnetic field gradient (dH/dx), ranged from 0.1441 – 0.1885 for ASSAB 705, 0.1373 – 0.1421 for ASSAB 709 and 0.1886 – 0.2225 for ASSAB 760. The shape and steepness of the exponential curves were found to vary with the alloy composition of the steels, particularly the chromium (Cr) and nickel (Ni) contents, with the curve gradient increasing as the stress ratio increased for each material.

These findings highlight the importance of material composition in the magnetic response during fatigue crack growth, emphasizing that steels with higher alloying elements such as Nickel and Chromium tend to exhibit distinct MMM signal behaviours. This has practical implications for the application of MMM testing in structural health monitoring, as it underlines the necessity of calibrating MMM systems specifically for the steel grade and loading conditions. By accurately correlating MMM signals with crack growth, maintenance engineers can improve early damage detection, prevent catastrophic failures, and optimize inspection intervals. Furthermore, understanding how stress ratios affect MMM responses enables better prediction of component lifespan under cyclic loading, enhancing safety and reliability across various industries.

ACKNOWLEDGEMENT

The authors wish to extend their appreciation to Universiti Kebangsaan Malaysia for their support of this research project through the GGPM-2023-016 fund.

DECLARATION OF COMPETING INTEREST

None.

REFERENCES

Anggraini, L. 2017. Hardenability of ASSAB 760 steel during tempering for punch holder applications. Solid State Phenomena, 266: 13-18.

Arifin, A., Abdullah, S., Ariffin, A.K., Jamaludin, N. & Singh, S.S.K. 2022. Characterising the stress ratio effect for fatigue crack propagation parameters of SAE 1045 steel based on magnetic flux leakage. *Theoretical and Applied Fracture Mechanics* 121: 103514.

Ariffin, A., Meor Ahmad, M.I., Abdullah, S. & Wan Jusoh, W.Z. 2015. Detection of cracked position due to cyclic loading for ferromagnetic materials based on magnetic memory method. *Jurnal Teknologi* 75(7): 67–70.

Dubov, A. A. 1997. A study of metal properties using the method of magnetic memory. *Metal Science And Heat Treatment* 39(9): 401-405.

Dubov, A. A., Demin, E. A., Milyaev, A. I., & Steklov, O. A. 2002. Experience in monitoring the stress-strain state of gas pipelines using the metal magnetic memory method in comparison with traditional methods and means of stress testing. *Kontrol'. Diagn* 4:53-56.

Dubov, A., 2006. Principle features of metal magnetic memory method and inspection tools as compared to known magnetic NDT methods. *Cinde Journal* 27(3):16.

Dubov, A., Dubov, A., Marchenkov, A., & Kolokolnikov, S. 2020. Study of the structure and mechanical properties of engineering products made of austenitic martensitic steel, using the metal magnetic memory technique. *Welding in the World* 64(11):1887-1895.

Firdaus, S.M., Arifin, A., Abdullah, S., Singh, S.S.K., & Nor, N.M. 2023. Fatigue Life Assessment of API Steel Grade X65 Pipeline Using a Modified Basquin Parameter of the Magnetic Flux Leakage Signal. *Materials* 16(2): 464

Hou, N., Ding, N., Qu, S., Guo, W., Liu, L., Xu, N., & Wu, C.M.L. 2022. Failure modes, mechanisms and causes of shafts in mechanical equipment. *Engineering Failure Analysis* 136:106216.

Huang, H., Jiang, S., Liu, R., & Liu, Z. 2014a. Investigation of magnetic memory signals induced by dynamic bending load in fatigue crack propagation process of structural steel. *Journal of Nondestructive Evaluation* 33(3): 407–412.

Huang, H., Jiang, S., Wang, Y., Zhang, L., & Liu, Z. 2014b. Characterization of spontaneous magnetic signals induced by cyclic tensile stress in crack propagation stage. *Journal of Magnetism and Magnetic Materials* 365: 70–75.

Huang, H., Qian, Z., Yang, C., Han, G., & Liu, Z. 2017. Magnetic memory signals of ferromagnetic weldment induced by dynamic bending load. *Nondestructive Testing and Evaluation* 32(2):166-184.

Li, L., Wong, Y. S., Fuh, J. Y. H., & Lu, L. 2001. Effect of TiC in copper–tungsten electrodes on EDM performance. *Journal of Materials Processing Technology* 113(1-3): 563-567.

Lihong, D., Binshi, X., Shiyun, D., Qunzhi, C., & Dan, W. 2008. Variation of stress induced magnetic signals during tensile testing of ferromagnetic steels. *NDT &E International* 41(3):184-189.

Liu, B., Sun, J., He, L., Geng, H., & Yang, L. 2023. Quantitative study on internal detection signal of weak magnetic stress in oil and gas pipelines based on force-magnetic noncoaxial effect. *Measurement* 215: 112870.

Mutalib, N.A.A.A, Nor, N.M., Arifin, A., & Abdullah, S. 2025. The Need to Investigate the Behaviour of Reinforcement using a Metal Magnetic Memory. *Jurnal Kejuruteraan* 37(3): 1117-1130.

Ni, C., Hua, L., & Wang, X. 2018. Crack propagation analysis and fatigue life prediction for structural alloy steel based on metal magnetic memory testing. *Journal of Magnetism and Magnetic Materials* 462:144-152.

Sahadan, S.N., Abdullah, S., Arifin, A., & Singh, S.S.K. 2021. December. Assessing the magnetic flux leakage contraction parameters for the fatigue life prediction of SAE1045 steel specimens. *Structures* 34: 4077-4085.

Shen, G. T., Wu, Y., & Wang, Y. 2004. Investigation on metal magnetic memory signal of surface crack on welding scar in LPG tank. *Key Engineering Materials* 270:647-650).

Zhang, K., Zhang, J., Jin, W., Mao, J., Li, Q., & Xu, F. 2021. A novel method for characterizing the fatigue crack propagation of steel via the weak magnetic effect. *International Journal of Fatigue* 146:106166.

Zhang, P., Jin, K., & Zheng, X. 2020. Magneto-mechanical coupling model of ferromagnetic materials under fatigue loading and its application in metal magnetic memory method. *Journal of Magnetism and Magnetic Materials* 514:167167.

Zhou, W., Fan, J., Ni, J., & Liu, S. 2019. Variation of magnetic memory signals in fatigue crack initiation and propagation behavior. *Metals* 9(1): 89.